EFFECT OF LIQUID VISCOSITY ON LIQUID SIDE MASS TRANSFER COEFFICIENT AT VERTICAL FILM FLOW ON EXPANDED METAL SHEETS

Zdeněk Brož and Mirko Endršt

Institute of Chemical Process Fundamentals,
Czechoslovak Academy of Sciences, 165 02 Prague 6 - Suchdol

Received May 11th, 1982

Experimental results are presented on the effect of liquid viscosity on absorption rate of carbon dioxide into a liquid film flowing downward the vertical surface of expanded metal sheets. On basis of these results the conclusion has been reached that the Highbie model does not enable to predict the effect of kinematic viscosity on liquid side mass transfer coefficient k_1. The film-penetration model has been proposed where the existence of non-mixed region is assumed at the interface with the thickness ϑ and to it periodically incoming disturbances with the length scale of disturbance λ and characteristic Reynolds number of disturbance equal to one. On basis of experimental data were evaluated the dimensionless thicknesses of the film and penetration regions $\vartheta^+ = 0{\cdot}04$ and $\lambda^+ = 10{\cdot}6$. A good agreement of the measured and calculated values of the mass transfer coefficient k_1 were obtained for three types of expanded metal sheets of vertical pitch diagonal 10, 16 and 28 mm and nine liquids with kinematic viscosities within the range from 0·6 to 15·1 $\mu m^2 s^{-1}$.

In this study, which is closely related to the last one[1], is studied the effect of viscosity on liquid side mass transfer coefficient at vertical film flow downward the surface of metal mesh. Geometrical structure of expanded metal sheets (Fig. 1 and Table I) is causing intensive mixing of the liquid film and consequently, the mass transfer coefficient is several times larger than on the smooth plate. Simultaneously the liquid film on expanded metal sheets is more stable and better distributed than on the smooth vertical plate. Behaviour of the liquid film flowing on the metal mesh is in certain features similar to flow on artificially roughened plane surface, as is *e.g.* stated by Davies[2] (wave interference flow). Experimental studies on the effect of viscosity and liquid flow rate on coefficient k_1 on expanded metal sheets with different geometric structure makes possible to understand the effect of geometry on hydrodynamics and mass transfer and to differentiate between different models of mass transfer mechanism into the liquid film.

In the last study[1] has been proposed, on basis of experimental data on absorption of relatively insoluble gases into water, to correlate the liquid side mass transfer coefficient by use of the Highbie model[3]

$$k_1 = (4D/(\pi\Theta))^{1/2} \qquad (1)$$

while the exposure time Θ has been expressed by relation

$$\Theta = h/v \tag{2}$$

where h is a half of vertical pitch diagonal of expanded metal sheets and v is the mean velocity of liquid film.

TABLE I
Expanded metal sheets. Length dimensions are in mm

Specification		10 stainless steel	16 stainless steel	28 steel
Vertical pitch diagonal	$2h$	10	16·5	28·2
Horizontal pitch diagonal	n	4	5·5	8
Vertical mesh diagonal	m_1	7	11·5	22
Horizontal mesh diagonal	m_2	2·2	3·3	5·7
Metal thickness	t_1	0·5	0·5	0·8
Rib thickness	t_2	1·0	1·2	1·8
Thickness of expanded metal	t_3	1·6	2	2·1
Plate width	l	66	63	63
Length of liquid film	H	530	640	640
Ratio of geometric plate surface occupied by metal	$A_w/2Hl$	0·73	0·54	0·56

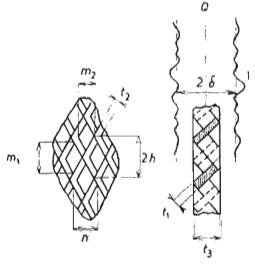

FIG. 1
Detail of expanded metal

Physically this means the assumption that complete mixing of liquid from the region of interface with the bulk of liquid takes place after a length equal to one half of the vertical pitch diagonal of the expanded metal sheets is passed. This assumption has been based on visual observation of the character of film flow. It has been observed that water flowing downward from the neighbouring ribs of the mesh of metal into the common point is causing turbulisation of liquid within the mesh of the metal. In the cited study a measurement has been performed of the absorption rate of three hard to dissolve gases *i.e.* of helium, carbon dioxide and propane into water at 25°C on three geometric dimensions of metal sheets. One plate of expanded metal with the width 63 or 65 mm was situated in the absorption cell while the length of liquid film was at maximum 670 mm. At high linear wetting density the water film has covered the whole geometric surface area of the expanded metal sheet while at low wetting densities the mesh of expanded metal were filled only partially and liquid was flowing mostly on the ribs of expanded metal. Therefore beside measurements of physical absorption of gas into water measurements of interfacial area by the chemical method were also performed. Carbon dioxide was absorbed at lowered pressure into aqueous solution of sodium hydroxide under the conditions of pseudofirst order kinetics. Measured interfacial liquid areas A were expressed as the ratio α of geometric areas of both sides of the metal sheets

$$\alpha = A/(2Hl) . \qquad (3)$$

The ratio α increases with increasing linear wetting density from $\alpha = 0{\cdot}4$ to $\alpha = 1-1{\cdot}08$, when the surface of expanded metal is covered by a continuous liquid film. From independently measured values $k_1\alpha$ and α was calculated in the last study the coefficient k_1. Comparison of measured with calculated values has revealed that for the case of gas absorption into water relations (*1*) and (*2*) are satisfactorily describing the dependence of mass transfer coefficient on linear wetting density, diffusivity and dimensions of expanded metal sheets.

EXPERIMENTAL

Experimental unit and measuring procedure for the mass transfer coefficient was described in detail in the last study[1]. Here is briefly characterised the used experimental unit and are described the made changes. In between the upper and lower vessels circulated about 60 to 100 liters of liquid. According to recommendations by Chung and Mills[4] a filter was fixed into the circulation loop with active carbon for removal of surface active compounds. Degassing of liquid in preceeding the experiment lasted four hours and was performed by spraying liquid at 5 kPa into the upper vessel. Before the measurement all liquid had been pumped into the upper vessel from where it was flowing at atmospheric pressure by free fall over a rotameter into the absorption cell having the dimensions $80 \times 16 \times 750$ mm. One sheet of expanded metal was situated in the absorption cell and liquid from the cell outlet was flowing through an overflow into the lower vessel. The absorption rate has been calculated from flow rate of humidified carbon dioxide measured by laboratory gas flowmeter and gas burette.

Physical properties of used liquids are summarised in Table II. Density and kinematic viscosity of solutions of ethyleneglycol in water at 25°C were measured by digital densitometer DMAO2C of Co Paar and viscometer Ubbelohde. Density, viscosity and surface tension of water at different temperatures were found in tables, from original studies of various authors were taken diffusivity[5-11,12] and solubility[13]. For aqueous solutions of ethyleneglycol with varying mole fraction was the surface tension found in Tables[14] or taken from original studies[4]. Solubility[4,15] and diffusivity[4,15,16] from original studies of different authors were plotted into a graph in de-

TABLE II

Physical properties of used liquids, empirical constants a, b (Eq. (6)) and minimum Reynolds numbers

Quantity	Water, °C			Mixture ethyleneglycol–water at 25°C					X, mol/mol
	45	25	13	0·082	0·11	0·21	0·30	0·54	0·97
$\nu \cdot 10^6$ $m^2 s^{-1}$	0·605	0·896	1·204	1·53	1·86	2·84	3·93	7·71	15·1
ϱ $kg m^{-3}$	990	997	994	1 026	1 035	1 056	1 072	1 094	1 107
$\sigma \cdot 10^3$ $N m^{-1}$	69·6	72·0	73·6	63	61·5	57·5	54	49	45
$\mathscr{H} \cdot 10^{-7}$ Pa	26·2	16·6	11·7	16·4	16·3	14·9	13·8	9·58	4·89
$D \cdot 10^9$ $m^2 s^{-1}$	3·03	1·95	1·40	1·45	1·30	1·00	0·80	0·60	0·32
Sc —	200	453	860	1 055	1 430	2 840	4 910	12 850	47 190
a, expanded metal 10	0·555	0·544	0·519	0·585	0·601	0·604	0·652	0·664	0·685
16	0·387	0·328	0·387	0·363	0·363	0·363	0·363	0·383	0·383
28	0·306	0·306	0·306	0·306	0·306	0·306	0·306	0·306	0·381
b, expanded metal 10	0·466	0·460	0·466	0·450	0·427	0·426	0·409	0·396	0·386
16	0·491	0·508	0·491	0·490	0·490	0·490	0·490	0·475	0·475
28	0·498	0·498	0·498	0·498	0·498	0·498	0·498	0·498	0·448
$Re(\alpha \sim 1)$, expanded metal 10	700	510	360	240	180	100	70	30	10
16	1 200	700	530	330	290	140	125	60	20
28	1 600	980	820	650	470	300	200	85	40

pendence on mole fraction of ethyleneglycol and from them were for the corresponding compositions read off the average values given in Table II.

Mass transfer coefficient $k_1\alpha$ was calculated by use of relation

$$k_1\alpha = (\Gamma/\varrho H) \ln (1/(1 - c_{b2}/c_w)) . \tag{4}$$

It was verified by testing experiments that degassing of liquid was sufficient and thus for the inlet concentration $c_{b1} = 0$ was substituted into relation (*4*). Moreover plug flow of liquid was assumed and independence of k_1 and α along the liquid film. Details on determination of the outlet concentration c_{b2} and concentration on interface c_w are described in the last study[1].

For determination of the mean velocity of liquid film v, needed in Eq. (*2*) an independent experiment has been proposed. From the difference of mass of the wetted and dry plate of expanded metal sheet hanged on a balance, liquid density and plate dimensions was determined the mean thickness of liquid film δ and this was substituted into relation (*5*) for calculation of the mean liquid film velocity

$$v = \Gamma/(\varrho\delta) . \tag{5}$$

Measured thickness of liquid film was correlated in the form

$$\delta(g/\nu^2)^{1/3} = a\, Re^b . \tag{6}$$

In Table II are given empirical constants a and b and also minimum values of Reynolds numbers for which, on basis of visual observations of the number of not filled mesh of metal plates, there holds $\alpha \geqq 0{\cdot}95$. The Reynolds number has been defined in the usual manner

$$Re = 4\Gamma/\mu . \tag{7}$$

Definition of the linear wetting density Γ and film thickness δ result from Eq. (*8*) and Fig. 1

$$\Gamma = Q\varrho/(2l) . \tag{8}$$

So selected definitions enable comparison with film thicknesses and coefficient k_1 obtained on the smooth plate. In both cases are numerical values of interfacial area on expanded metal and on the smooth plate identical (when $\alpha \sim 1$). Measuring procedure, results and discussion of hydrodynamics of vertical liquid film flow on expanded metal is for wider range of physical properties of liquid presented in the next paper of this series.

RESULTS

Penetration Model by Highbie

Measured mass transfer coefficients of individual liquids are compared in Figs 2 to 4 with values calculated from equation based on penetration model

$$k_1 = g^{1/6}\nu^{2/3} Re^{(1-b)/2} / (\pi h a Sc)^{1/2} \tag{9}$$

Eq. (9) has been obtained by substituting the values from Eqs (2), (5), (6), and (7) into Eq. (1). In Fig. 2 are plotted experimental data of all nine liquids summarised in Table II. In Figs 3 and 4 were plotted for simplicity experimental points of only five liquids with kinematic viscosities $\nu = 0{\cdot}605$, $0{\cdot}896$ (water at 45 and 25°C), $2{\cdot}84$, $7{\cdot}71$ and $15{\cdot}1\ \mu m^2 s^{-1}$ (mixtures of ethyleneglycol with water). From these figures is obvious that measured values of k_1 for low viscosity liquids and expanded metal sheets 10 and 16 mm are in a good agreement with values predicted according to Eq. (9). This is in agreement with the earlier obtained results[1] of absorption of gases into water at 25°C. Moreover here are for film thicknesses used directly measured values instead of the earlier used values which were calculated from the correlation relation[5] for a pack of parallel plates. With expanded metal 28 mm the calculated k_1 values even for water are significantly lower than those measured. Better fit would be obtained by choosing a lower value of h in Eq. (9). For liquids with higher kinematic viscosity are the calculated values of coefficient k_1 systematically higher than the experimental values for all used dimensions of expanded metal. As the half of vertical pitch diagonal of expanded metal h is defined by geometry of expanded metal, relation (9) does not contain for k_1 any adjustable parameter.

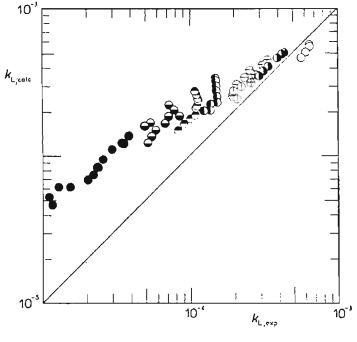

FIG. 2

Comparison of experimental and calculated from Eq. (9) values of k_1 for expanded metal 10 mm. ν ($\mu m^2 s^{-1}$): ○ 0·605, ◑ 0·896, ⊕ 1·204, ⊙ 1·53, ⊖ 1·86, ◐ 2·84, ◓ 3·93, ◒ 7·71, ● 15·1

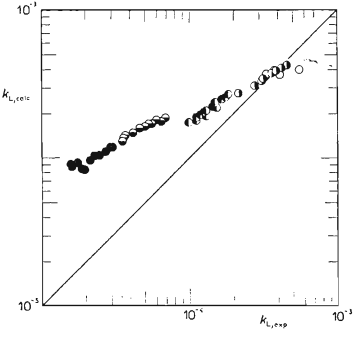

FIG. 3

Comparison of experimental and calculated from Eq. (9) values of k_1 for expanded metal 16 mm. ν ($\mu m^2 s^{-1}$): ○ 0·605, ◑ 0·896, ◐ 2·84, ◒ 7·71, ● 15·1

From Figs 2 to 4 is thus obvious that the penetration model is not predicting correctly first of all the effect of kinematic viscosity of liquid on coefficient k_1. Some idea on how large should be the distance of "full liquid mixing" from the region of interface with the bulk of liquid for different values of Reynolds number and liquid viscosity can be obtained by arranging Eq. (*1*) into the form

$$h_{calc} = (4D\Gamma/(\pi\varrho\delta k_1^2))^{1/2} . \qquad (10)$$

The calculated value h_{calc} must be now considered as an adjustable parameter of the penetration model. Its dependence on Reynolds number is presented in Figs 5 and 6 for expanded metals 10 and 28 mm. At low values of kinematic liquid viscosity the calculated values h_{calc} correspond to expected values and they do not depend on Reynolds number at all or very little. At the rise of kinematic viscosity also increases the value h_{calc}. "Complete mixing" thus takes place at a greater vertical distance than is half of vertical pitch diagonal of expanded metal h. The shape of dependence of h_{calc} on Reynolds number of liquid is complex and depends not only on viscosity but also on dimensions of expanded metal. For example for expanded metal 28 mm decreases h_{calc} with increasing Reynolds number practically at all viscosities. For expanded metal 10 mm at very low and high liquid viscosities h_{calc} does not depend on Reynolds number, at the mean liquid viscosities it at first decreases and then increases with increasing Reynolds number. It is obvious that it is not possible to expect existence of a simple corrective function for the dependence of h_{calc} on Reynolds number, liquid viscosity and expanded metal dimensions.

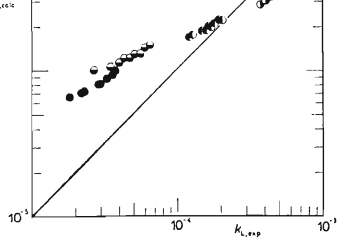

FIG. 4

Comparison of experimental and calculated from Eq. (*9*) values of k_1 for expanded metal 28 mm. Experimental points are denoted as those in Fig. 3

In Fig. 7 are given dependences of the liquid side side mass transfer coefficient k_1, adjustable parameter h_{calc} and film thickness on Reynolds number for individual expanded metal sheets at kinematic viscosity $\nu = 2{\cdot}84 \,.\, 10^{-6}\ m^2\ s^{-1}$. Solid lines represent experimental points, actually measured coefficients k_1 as experimental points are plotted *e.g.* in Figs 10–12. Empty points on curves denote minimum Reynolds numbers at which the value $\alpha \sim 1$ has been reached according to visual observations. It is obvious from Fig. 7 that coefficients k_1 increase with the Reynolds number for expanded metals of 16 and 28 mm in the whole range of Reynolds numbers while with expanded metal of 10 mm the maximum is reached with following slow decrease of coefficient k_1. For comparison is also plotted the dependence obtained by Chung and Mills[4] on smooth plate at absorption of carbon dioxide into solutions of ethyleneglycol in water with kinematic viscosity $\nu = 2{\cdot}75 \,.\, 10^{-6}\ m^2\ .\ s^{-1}$. This dependence has for smooth plate at $Re = 1\,200$ a characteristic transition regime of laminar wavy flow into the turbulent flow. According to relations recommended by Bakopoulus[6] and Brauer[7] for coefficients k_1 of smooth pipe in the laminar, transition and turbulent regions has been plotted line *5* with transitions between the regions at $Re = 280$ and 1 600. From Fig. 7 results that all expanded metals have, due to their spatial structure, larger values of k_1 already at low Reynolds numbers for liquid which is as regards the practical application especially advantageous.

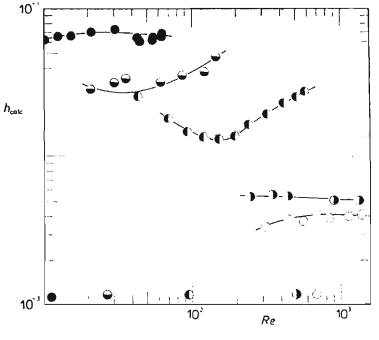

FIG. 5

Adjustable parameter h_{calc} (Eq. (*10*)) in dependence on Reynolds number for expanded metal 10 mm. Experimental points are denoted as those in Fig. 3. Solid lines were drawn through experimental points

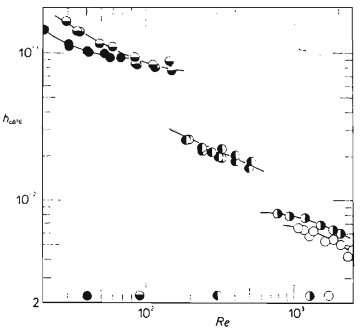

FIG. 6

Adjustable parameter h_{calc} (Eq. (*10*)) in dependence on Reynolds number of expanded metal 28 mm. Experimental points are denoted as those in Fig. 3. Solid lines were drawn through experimental points

Character of dependence of the coefficient k_1 on Re of the smooth plate in the region of laminar wavy flow is the closest dependence for expanded metal of 10 mm. Of all expanded metals the one of 10 mm is closest to the smooth plate also as regards the geometric structure and hydrodynamics of film flow. Its large number of mesh of small dimensions and large part of geometrical area occupied by metal $A_w/2111$ (Table I) results in greater thickness of liquid film δ (Fig. 7) at the same Reynolds number. More frequent disturbances caused by individual meshes have obviously a smaller amplitude and for viscous liquids also a smaller probability to penetrate toward the interface and to mix the liquid from the bulk to interface. By this procedure it is possible to explain qualitatively the dependence both of coefficient k_1 as well as of the adjustable parameter h_{calc} on Reynolds number of liquid, viscosity and dimensions of expanded metal sheets. As has been already mentioned it is not advisable to substitute for the geometric dimension h in the penetration model (vertical pitch diagonal of expanded metal) the adjustable parameter h_{calc} due to its obviously complex dependence on dimensions of expanded metal, viscosity and Reynolds number of liquid.

Film-Penetration Model

Above made evaluation of experimental data on coefficient k_1 based on the penetration model has led to the idea on possible use of the film-penetration model for description of the mass transfer mechanism from the moving interface into the bulk of liquid phase. In literature can be found experimental proofs on dumping effect of liquid interface on disturbances arriving from the bulk of liquid phase[7,8]. Let us thus assume that the interface behaves as semirigid and that periodically arriving

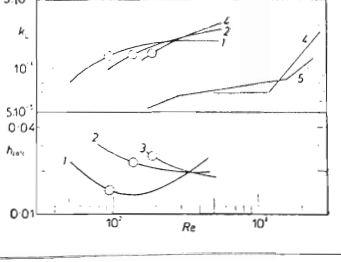

FIG. 7

Coefficient k_1, adjustable parameter h_{calc} and liquid film thickness δ in dependence on Reynolds number for kinematic viscosity $\nu = 2{\cdot}84 \cdot 10^{-6}$ m^2 s^{-1}. *1* Expanded metal 10 mm, *2* 16 mm, *3* 28 mm, *4* Chung and Mills[4] measurement on smooth pipe $\nu = 2{\cdot}75 \cdot 10^{-6}$ m^2 s^{-1}, *5* Brauer[7] and Bakopoulos[6] correlation for smooth pipe. ○ value of Reynolds number for liquids at $\alpha \approx 1$

disturbances with the linear scale λ penetrate only up to a distance ϑ from the interface. Let us also assume that the region of liquid with thickness ϑ is not exchanged with the bulk liquid and that steady diffusion there takes place. Disturbances with linear dimension λ coming from the liquid core remain at the boundary of this region for the time equal to the time scale of disturbance τ and during that time an unsteady mass transfer takes place. This is the usual scheme of film-penetration mechanism of mass transfer. From the model by Kolář[9] describing the interfacial heat and mass transfer in turbulent flow is used the assumption on relation between the length and time scale of disturbances in the transition regions. According to the made assumption the Reynolds number of disturbance is equal to one

$$Re_\lambda = v_\lambda \lambda / \nu = 1 \tag{11}$$

and the characteristic dimension of the disturbance is equal to the magnitude of this region. For the time scale of disturbance then results the relation

$$\tau = \lambda^2 / \nu . \tag{12}$$

The film-penetration model then has the form

$$k_1 = D/(\vartheta + \sqrt{(\pi)}\lambda/(2Sc^{1/2})) \tag{13}$$

which for $\vartheta = 0$ corresponds to the penetration model[3] and for $\lambda = 0$ to the film model[10]. Let us also assume that the dimension of regions ϑ and λ depends on the friction velocity

$$u^* = (\tau_w/\varrho)^{1/2} \tag{14}$$

similarly as with the single phase flow in the channel the relations

$$\vartheta = \vartheta^+ \nu / u^* \quad \text{and} \quad \lambda = \lambda^+ \nu / u^* \tag{15a,b}$$

include dimensionless thickness of regions ϑ^+ and λ^+. The shear stress on the wall of expanded metal τ_w results directly from relation

$$\tau_w A_w = 2\varrho g \delta H l \tag{16}$$

in which A_w represents total surface area of the metal plate with the plate width l and length H. Eq. (13) can be written in the form

$$k_1 = u^*/[Sc\vartheta^+ + (\sqrt{(\pi)}/2)\,\lambda^+ Sc^{1/2}] \tag{17}$$

or after substitution for friction velocity u^* into the form

$$k_L = \frac{(2Hl\,a/A_w)^{1/2}\, Re^{b/2}(gv)^{1/3}}{Sc\,\vartheta^+ + (\sqrt{(\pi)}/2)\,\lambda^+\, Sc^{1/2}} \,. \qquad (18)$$

In Fig. 8 is plotted the dependence of coefficient k_L on friction velocity u^* given by Eq. (17) for two kinematic liquid viscosities and individual dimensions of expanded metal. Straight lines passing through the origin were calculated by use of parameters $\vartheta^+ = 0{\cdot}04$ and $\lambda^+ = 10{\cdot}6$ evaluated later on. Lower values of friction velocities $u^* < 0{\cdot}05$ cannot be reached because at small values of Reynolds number significantly decreases the value of α below the value $\alpha \approx 1$. It is obvious that agreement with relation (17) is good.

Dimensionless hydrodynamic parameters of the model ϑ^+ and λ^+ can be obtained from experimental data by arranging Eq. (17) into the form

$$u^*/(k_L Sc) = \vartheta^+ + \lambda^+(\sqrt{(\pi)}/2)\,Sc^{-1/2} \qquad (19)$$

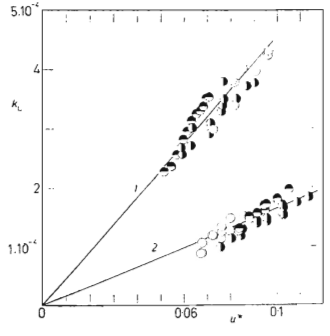

FIG. 8

Coefficient k_L in dependence on friction velocity u^*. *1* $\nu = 0{\cdot}896 \,.\, 10^{-6}\ m^2\ s^{-1}$, *2* $\nu = 2{\cdot}84 \,.\, 10^{-6}\ m^2\ s^{-1}$. ○ expanded metal 10 mm, ◑ 16 mm, ◓ 28 mm

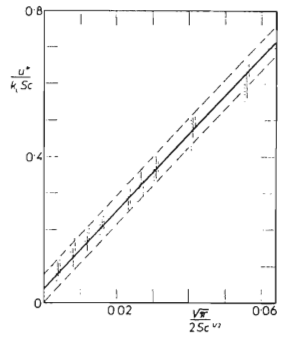

FIG. 9

Evaluation of ϑ^+ and λ^+ from experimental data. Slope of straight line $\lambda^+ = 10{\cdot}6$. Intercept with *y*-axis: *1* $\vartheta^+ = 0{\cdot}08$, *2* $\vartheta^+ = 0{\cdot}04$ and *3* $\vartheta^+ = 0$. ——— Expanded metal 10 mm, – – – – 16 mm, ····· 28 mm

From Fig. 9 is obvious that experimental data of all dimensions of expanded metal form a unique dependence through which can be plotted a straight line with the slope $\lambda^+ = 10{\cdot}6$ and y-axis intercept $\vartheta^+ = 0{\cdot}04$. In this figure are also plotted two other straight lines $\vartheta^+ = 0$ and $\vartheta^+ = 0{\cdot}08$ which approximately form a lower and upper limits of experimental data.

In Figs 10 – 12 are given experimental data of the mass transfer coefficient k_l in dependence on Reynolds number of liquid. Solid lines are calculated from Eq. (*18*) after substitution for $\vartheta^+ = 0{\cdot}04$ and $\lambda^+ = 10{\cdot}6$, dashed lines are calculated for two viscosities according to Eq. (*9*) of the penetration model. It is obvious that Eq. (*18*) fits well the dependence of k_l on Reynolds number and on viscosity for all dimensions of expanded metal.

DISCUSSION

Relations (*9*) and (*18*) derived for the liquid side mass transfer coefficient k_l on basis of the penetration and film-penetration models differ first in parameters characterising expanded metal geometric structure and second in numerical values of gravitational acceleration, kinematic viscosity, Schmidt and Reynolds number exponents.

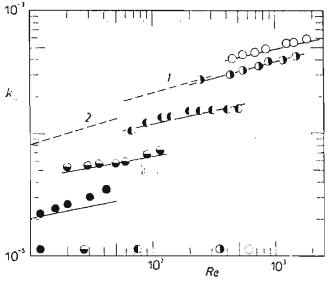

FIG. 10

Coefficient k_l in dependence on *Re* for expanded metal 10 mm. Experimental points are denoted as those in Fig. 3. ——— Film-penetration model Eq. (*18*), – – – penetration model Eq. (*9*). *1* $\nu = 2{\cdot}84 \cdot 10^{-6}\ m^2 \cdot s^{-1}$, *2* $\nu = 15{\cdot}1 \cdot 10^{-6}\ m^2\ s^{-1}$. On x-axis are denoted points having $\alpha \approx 1$

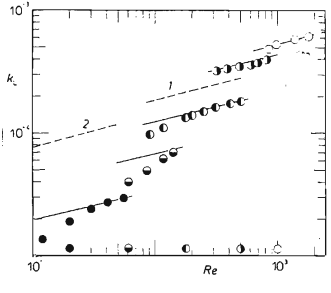

FIG. 11

Coefficient k_l in dependence on *Re* number for expanded metal 16 mm. Used symbols are the same as those in Fig. 10

In the case of Reynolds number the difference between the exponents according to the penetration and film-penetration models is small. This results from the fact that the numerical value of exponent b in relation (6) for the thickness of the liquid film is within the range $b = 0{\cdot}386 - 0{\cdot}398$ (Table II) and thus the calculated values of exponents $(1 - b)/2$ and $b/2$ differ very little. This is obvious also from comparison of slopes of dependences of the coefficient k_1 on Reynolds number demonstrated in Figs 10 and 11 for kinematic viscosities $\nu = 2{\cdot}84 \cdot 10^{-6}$ and $15{\cdot}1 \cdot 10^{-6}$ m^2 s^{-1} by solid and dashed lines. The exponent of dependence k_1 on Reynolds number thus does not enable to distinguish both models.

Difference between exponents of the dependence of coefficient k_1 on kinematic viscosity is very significant. Exponent of the dependence according to the penetration model has the value equal to 2/3 and according to the film-penetration model to 1/3. Their effect on coefficient k_1 is obvious from Figs 10 and 11 from comparison of values given by the dashed line (penetration model) and by the solid line (film-penetration model).

In Fig. 13 is plotted the dependence of dimensionless mass transfer coefficient k_1/u^* on Schmidt number for dimensionless hydrodynamic parameters ϑ^+ and λ^+ calculated on basis of Fig. 9, *i.e.* for $\lambda^+ = 10{\cdot}6$ and different values of $\vartheta^+ = 0$, 0·04 and 0·08. For the value $\vartheta^+ = 0$ the straight line has the slope equal to $-1/2$ which is characteristic for the penetration model. From the curved dependence for $\vartheta^+ = 0{\cdot}04$ and 0·08 of the film-penetration model results that the exponent of the dependence of k_1 on Schmidt number depends both on values of ϑ^+ and λ^+ as well as on the value of the Schmidt number and the exponent is within the range $-1/2$ to -1. Our experimental data could not prove the dependence in Fig. 13 as the change in Schmidt number were reached by changing the liquid viscosity on which depended both the gas diffusivity in liquid as well as the hydrodynamics of the film flow (Ta-

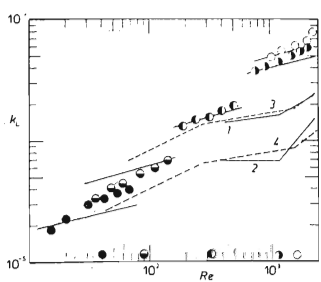

FIG. 12

Coefficient k_1 in dependence on Re number for expanded metal 28 mm. Experimental points are denoted as those in Fig. 3. ——— Smooth pipe, measurements by Chung and Mills[4]. *1* $\nu = 0{\cdot}661 \cdot 10^{-6}$ m^2 s^{-1}, *2* $\nu = 2{\cdot}75 \cdot 10^{-6}$ m^2 s^{-1}. – – – – – smooth pipe, correlation by Brauer[7] and Bakopoulos[6] *3* $\nu = 0{\cdot}661 \cdot 10^{-6}$ m^2 s^{-1}, *4* $\nu = 2{\cdot}75 \cdot 10^{-6}$ m^2 s^{-1}

ble II). It was also not possible to study the exponent of the effect of gravitational acceleration.

As results from Fig. 13, effect of dimensionless thickness of the non-mixed region ϑ^+ on coefficient k_1 is significant especially at high values of Schmidt numbers. For value of parameter $\lambda^+ = 10{\cdot}6$ are given in Table III the calculated ratios of coeffi-

TABLE III

Ratio $k_1(\vartheta^+ = 0)/k_1(\vartheta)^+$ in dependence on Schmidt number

Sc	$k_1(\vartheta^+ = 0)/k_1(\vartheta^+ = 0{\cdot}04)$	$k_1(\vartheta^+ = 0)/k_1(\vartheta^+ = 0{\cdot}08)$
10^2	1·043	1·085
10^3	1·14	1·27
10^4	1·43	1·85
10^5	2·35	3·69

TABLE IV

Effect of Reynolds number on ratio ϑ/δ and λ/δ for expanded metal sheet 10 mm

Re	ϑ/δ	λ/δ
10	0·018	4·7
100	0·0037	0·99
1 000	0·00079	0·21

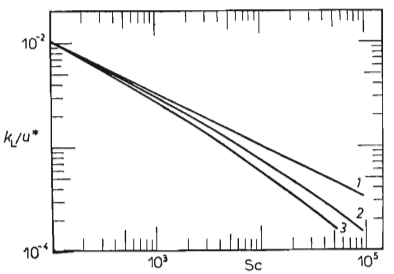

FIG. 13

Ratio k_1/u^* in dependence on Schmidt number for $\lambda^+ = 10{\cdot}6$. *1* $\vartheta^+ = 0$, *2* $\vartheta^+ = 0{\cdot}04$, *3* $\vartheta^+ = 0{\cdot}08$

cients k_l ($\vartheta^+ = 0$) and k_l ($\vartheta^+ = 0{\cdot}04$) or k_l ($\vartheta^+ = 0{\cdot}08$) and it is obvious that higher value ϑ^+ is causing decrease of k_l. What is the "actual" thickness of the non-mixed region ϑ can be evaluated by substituting the friction velocity u^* into Eq. (*15a*). But most advantageous is to express ϑ as the ratio in relation to the thickness of the liquid film δ. At use of Eq. (*6*) and (*15a*) for the ratio ϑ/δ the relation is obtained

$$\vartheta/\delta = \vartheta^+ (A_w/(2Hl))^{1/2}/(a\ Re^h)^{3/2} . \qquad (20)$$

Similarly it is also possible to obtain the relation for λ/δ. From calculated values given in Table IV results that the thickness of the nonmixed region ϑ, in which is assumed the existence of steady diffusion, forms a relatively small part of thickness of liquid film δ, especially at large values of the Reynolds number of liquid. Contrary to values ϑ/δ are the ratios λ/δ rather too high. At small Reynolds numbers, when the ratio λ/δ is the highest, physical interpretation would suggest to consider distorted disturbances which have longer axis directed parallel to interface rather than across the liquid film thickness δ. Certain improvement is obtained, when the existence of only one disturbance in the bed of liquid with thickness 2δ is assumed. The disturbance with the characteristic dimension λ would be then limited on both sides by the thickness of the non-mixed region of the film ϑ.

The film-penetration model represents similarly as the penetration model a certain simplified description of mechanism of mass transfer from the interface into the bulk of liquid. Its advantage is an elementary mathematic description of the given physical conception and simple interpretation of experimental data. Two adjustable parameters of the model ϑ^+ and λ^+ represent dimensionless thicknesses of defined hydrodynamic regions and enable to correlate all experimental data in a wide range of flow rates and physical properties of liquids and geometrical structures of expanded metal sheets.

LIST OF SYMBOLS

a empirical constant in Eq. (*9*) (—)
A interfacial area on the expanded metal sheet (m^2)
A_w geometric surface area of metal on the expanded metal sheet (m^2)
b empirical constant in Eq. (*6*) (—)
c_b concentration in bulk of liquid ($mol\ m^{-3}$)
c_w concentration at interface ($mol\ m^{-3}$)
D diffusivity of gas in liquid ($m^2\ s^{-1}$)
g gravitational acceleration ($m\ s^{-2}$)
h half of the vertical pitch diagonal (m)
h_{calc} adjustable parameter in Eq. (*10*) (m)
H length of liquid film (m)
$\mathscr{H}$ Henry's law constant (Pa)
k_l liquid side mass transfer coefficient ($m\ s^{-1}$)

l width of expanded metal sheet (m)
Q volumetric flow rate of liquid ($m^3 s^{-1}$)
Re Reynolds number of liquid film (—)
Re_λ characteristic Reynolds number of disturbance (—)
Sc Schmidt number (—)
u^* friction velocity defined by Eq. (*14*) ($m s^{-1}$)
v mean velocity of liquid film defined by Eq. (*5*) ($m s^{-1}$)
v_λ velocity scale of disturbance ($m s^{-1}$)
x mole fraction of ethyleneglycol (—)
α relative interfacial area defined by Eq. (*3*) (—)
Γ linear wetting density defined by Eq. (*8*) ($kg m^{-1} s^{-1}$)
δ mean thickness of liquid film (Fig. 1) (m)
Θ exposure time according to the penetration model, defined by Eq. (*2*) (s)
ϑ thickness of the non-mixed region at interface (m)
ϑ^+ dimensionless thickness of non-mixed region, Eq, (*15a*) (—)
λ length scale of disturbance (m)
λ^+ dimensionless length scale of disturbance, Eq. (*15b*) (—)
μ dynamic viscosity ($kg m^{-1} s^{-1}$)
ν kinematic viscosity ($m^2 s^{-1}$)
ϱ density ($kg m^{-3}$)
σ surface tension ($N m^{-1}$)
τ time scale of disturbance defined by Eq. (*12*) (s)
τ_w shear stress on the wall of expanded metal sheets ($N m^{-2}$)

REFERENCES

1. Brož Z., Endršt M.: This Journal *45*, 3089 (1980).
2. Davies J. T.: *Turbulence Phenomena*. Academic Press, New York 1972.
3. Higbie R.: Trans. AIChE *31*, 365 (1935).
4. Chung D. K., Mills A. F.: Int. J. Heat Mass Transfer *19*, 51 (1976).
5. Tesař A., Kolář V.: This Journal *42*, 3301 (1977).
6. Bakopoulos A.: Ger. Chem. Eng. *3*, 241 (1980).
7. Brauer H.: Ger. Chem. Eng. *3*, 149 (1980).
8. Davies J. T., Lozano F. J.: AIChE J. *25*, 405 (1979).
9. Kolář V.: This Journal *42*, 1310 (1977).
10. Lewis W. K., Whitman W. G.: Ing. Eng. Chem. *16*, 1215 (1924).
11. Nijsing R. A. T. O., Hendriksz R. H., Kramers H.: Chem. Eng. Sci. *10*, 88 (1969).
12. Thomas W. J., Adams H. J.: Trans. Faraday Soc. *61*, 668 (1965).
13. Wilhelm E., Battino R., Wilcock J.: Chem. Rev. *77*, 219 (1977).
14. *Handbuch des Chemikers*, p. 786. Verlag Technik, Berlin 1956.
15. Hayduk W., Malik V. K.: Chem. Eng. Data *16*, No 2, 143 (1971).
16. Calderbank P. H.: Trans. Inst. Chem. Engr. *37*, 179 (1959).

Translated by M. Rylek